NJC

New Journal of Chemistry

rsc.li/njc

A journal for new directions in chemistry

ROYAL SOCIETY
OF CHEMISTRY

PAPER
Iti Gupta *et al.*
Visible light assisted oxidation of organic compounds by
iridium(III)dipyrrinato complexes

CNRS

Check for updates

Visible light assisted oxidation of organic compounds by iridium(III)dipyrrinato complexes†

Shekhar Kumar, [iD] Lalita Devi [iD] and Iti Gupta [iD] *

Photo-assisted oxidation of organic compounds is a greener and more sustainable approach, which utilizes a very small amount of photocatalyst and visible light or sunlight. Ir(III) cyclometalated complexes have been explored extensively for photocatalytic applications in the past. Alternatively, Ir(III)dipyrrinato complexes can be employed for photocatalysis as they have attractive optical properties with high singlet oxygen generation ability. An efficient protocol for the photocatalytic aerobic oxidation of amines and sulfides by utilizing only 0.05 mol% Ir(III)dipyrrinato complexes is reported. The reactions are completed in 2 hours, providing imines and sulfoxides, in excellent yields. Additionally, a methodology for the hydroxylation of aryl boronic acids using 0.05 mol% Ir(III)dipyrrinato catalyst is reported. These methods display excellent substrate tolerance and offer an effective strategy for synthesizing a diverse range of functionalized imines, sulfoxides and phenols in a highly efficient manner, which validates the versatility of Ir(III)dipyrrinato complexes as photocatalysts for various organic transformations. Notably, these photochemical transformations require only a minimal catalyst loading of 0.05 mol% for these reactions, which demonstrates their exceptional cost-effectiveness.

Introduction

The oxidation of organic compounds plays an important role in organic synthesis. Compounds such as imines, phenols and sulfoxides are very important classes of compounds. Imines are key intermediates to synthesize many fine chemicals, dyes and pharmaceutical drugs.[1,2] The condensation between primary amines and carbonyl compounds leads to the formation of imines, but the high reactivity of carbonyl compounds leads to the formation of unwanted products. Phenols are frequently occurring scaffolds in biologically active compounds such as natural products and pharmaceuticals.[3] They are also key intermediates in organic synthesis.[4,5] Phenols are traditionally synthesized through nucleophilic aromatic substitution on aryl halides containing electron-withdrawing groups, as well as by the hydrolysis of arene diazonium salts. However, this method has very poor functional group tolerance, which leads to a limited substrate scope.[6] Sulfoxides are crucial intermediates in organic synthesis[7–10] and are also present in many pharmaceutical drugs, such as omeprazole, modafinil, sulindac, sulforaphane and fipronil.[1,11,12] Traditionally, strong oxidizing agents, such as *m*-CPBA,[13,14] 2-iodobenzoic acid (IBX),[15] or Oxone,[16] are

needed for sulfoxidation, and in many cases, high temperatures and high reaction times are also required. These harsh conditions result in the over-oxidation of the sulfide to a sulfone.

The above-mentioned issues necessitate the development of efficient, sustainable and selective oxidation strategies. In recent years, visible-light assisted photocatalysis has emerged as an efficient and environmentally benign approach for the synthesis of fine chemicals.[17–20] Given its high natural abundance and clean energy profile, visible-light-driven photocatalysis is a promising alternative to traditional oxidation methods.[12,17,21–28] Molecular oxygen (O_2) is a widely available and environmentally friendly oxidant that can be employed in oxidative photocatalytic transformations, including the oxidative coupling of benzylamines to imines,[25,29–31] oxidation of sulfides to sulfoxides,[22,24,26–28,32] and oxidative hydroxylation of boronic acids to phenols.[23,33–37] However, challenges such as high catalyst loading and long reaction times often limit the practical application of these methodologies.

Metal-dipyrrinato complexes have recently garnered significant attention as efficient photocatalysts due to their high absorption coefficients in the visible region and long-lived triplet excited states, making them excellent photosensitizers.[38,39] In this work, we have utilized previously reported three *meso*-substituted Ir(III)dipyrrinato complexes and investigated their catalytic efficiency for a number of photocatalytic reactions for the first time. These complexes have a high absorption coefficient in visible light and high singlet oxygen quantum yield. We demonstrated the photocatalytic application of Ir(III)dipyrrinato

Indian Institute of Technology Gandhinagar, Palaj Campus, Gandhinagar, Gujarat-382355, India. E-mail: iti@iitgn.ac.in

† Electronic supplementary information (ESI) available: Characterization data such as ^{1}H NMR, ^{13}C NMR and ^{19}F-NMR of selected compounds. Singlet oxygen generation plots for **Ir1** and **Ir2**. See DOI: https://doi.org/10.1039/d5nj01795e

complexes using only 0.05 mole % catalytic loading for the oxidative coupling of benzylamine to an imine, conversion of sulfides to sulfoxides and oxidative hydroxylation of boronic acids to phenols.

Results and discussion

In this work, three Ir(III)dipyrrinato complexes (**Ir1**–**Ir3**) (as shown in Fig. 1) containing electron-donating and electron-withdrawing moieties at the C-5 position of the dipyrrin ligand (phenyl, *N*-butylcarbazole and pentafluorophenyl groups) were prepared as per the reported method and employed for photo-catalytic applications.[40,41]

Singlet oxygen generation

In the case of photocatalytic oxidation, molecular oxygen plays a crucial role as an oxidant. The generation of singlet oxygen became very important because it acts as one of the reagents in the reaction. Therefore, there is a significant demand for catalysts with exceptional singlet oxygen generation capability. A singlet oxygen generation experiment was conducted to determine the singlet oxygen quantum yields of the Ir(III)dipyrrinato complexes (**Ir1**, **Ir2** and **Ir3**) by following the standard protocol[42] using Rose Bengal[43] as the reference in methanol solvent.

Fig. 2 shows plots of the **Ir3** complex's singlet oxygen generation assay, whereas data for the **Ir1** and **Ir2** complexes can be found in the ESI† (Fig. S1). The figures show that **Ir3** produced a singlet oxygen quantum yield of 90%, while the **Ir1** and **Ir2** complexes produced singlet oxygen quantum yields of 87% and 81%, respectively.

Photo-oxidative benzylamine coupling

The excellent singlet oxygen quantum yield of these Ir(III)di-pyrrinato complexes encouraged us to utilize them as photo-sensitizers for various photo-oxidation reactions. At first, we tested them for the photo-oxidative benzylamine coupling reaction, and the reaction optimization results are summarized in Table 1.

When white light was used as an excitation source in acetonitrile (ACN), **Ir3** exhibited the highest catalytic efficiency and afforded **2a** in 97% yield (entry 1). Under the same conditions, **Ir2** and **Ir1** demonstrated moderate activity, yielding the desired product in 64% and 84% yield, respectively (entries 2 and 3). The reaction proceeded efficiently under natural sunlight, with a 97% yield (entry 4). The solvent effect

was further explored using **Ir3** as a photocatalyst under white light. When methanol (MeOH) and hexane were used as the solvent, the reaction yield dropped significantly to 23% and 25%, respectively (entries 5 and 6). Tetrahydrofuran (THF) and chloroform showed slightly improved performance, with yields of 32% and 54%, respectively (entries 7 and 8). The control experiments further confirmed the necessity of both the photo-catalyst and the light source. In the absence of a catalyst and light, the reaction in ACN afforded the product only in 3% and 2% yields, respectively (entries 9 and 10).

These optimization reactions suggest that **Ir3** works best for the photo-oxidative benzylamine coupling reaction in the presence of the white LED or sunlight and ACN solvent. A variety of substrate scopes were examined by utilizing the optimized reaction conditions (Scheme 1). In the case of unsubstituted benzylamine, the product (**2a**) yield was 97% under both the white LED and sunlight. Electron-donating substituents, such as *para*-methoxy and *ortho*-methyl groups, were well tolerated and afforded **2b** and **2c** products with very good yields in both sunlight and white light. In contrast, fluorine derivatives showed excellent conversion, including *para*-fluoro (**2d**, 94%/97%), *ortho*-fluoro (**2e**, 96%/95%) and trifluoromethyl (**2f**, 89%/92%), indicating strong compatibility with the reaction conditions, while *para*-substituted bromine (**2g**, 90%/92%) and chlorine (**2i**, 92%/94%) derivatives of benzylamine also yielded high conversions. However, *ortho*-substituted bromobenzylamine showed a decrease in reactivity, yielding product **2h** in only 59% yield under a white LED and 61% yield under sunlight, likely due to steric hindrance. However, in the case of secondary amines, dibenzylamine afforded **2a** with 96% yield and 1,2,3,4-tetrahydroisoquinoline also afforded the desired imine product **2j** with 67% and 65% yields under both white LEDs and sunlight, respectively.

Sulfoxidation

In the case of photocatalytic sulfoxidation, the influence of different parameters, such as catalyst, solvent and different light, was investigated to achieve high selectivity and conversion. For the optimization, methylphenyl sulfide (1 mmol, **3a**) was selected as the model substrate to assess the efficiency of the oxidation process. In all cases, molecular oxygen (O₂) was purged in the reaction mixture for 15 minutes and placed under an O₂ atmosphere to ensure a sufficient oxygen supply for the catalytic transformation. The effect of different solvents and
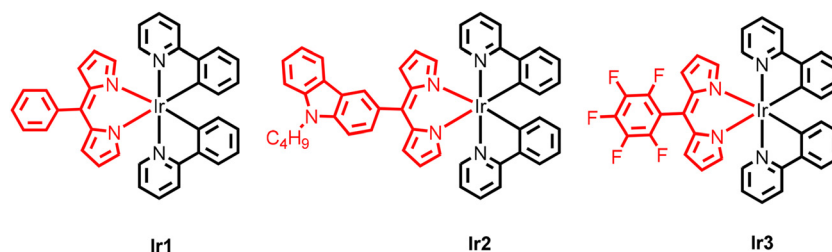

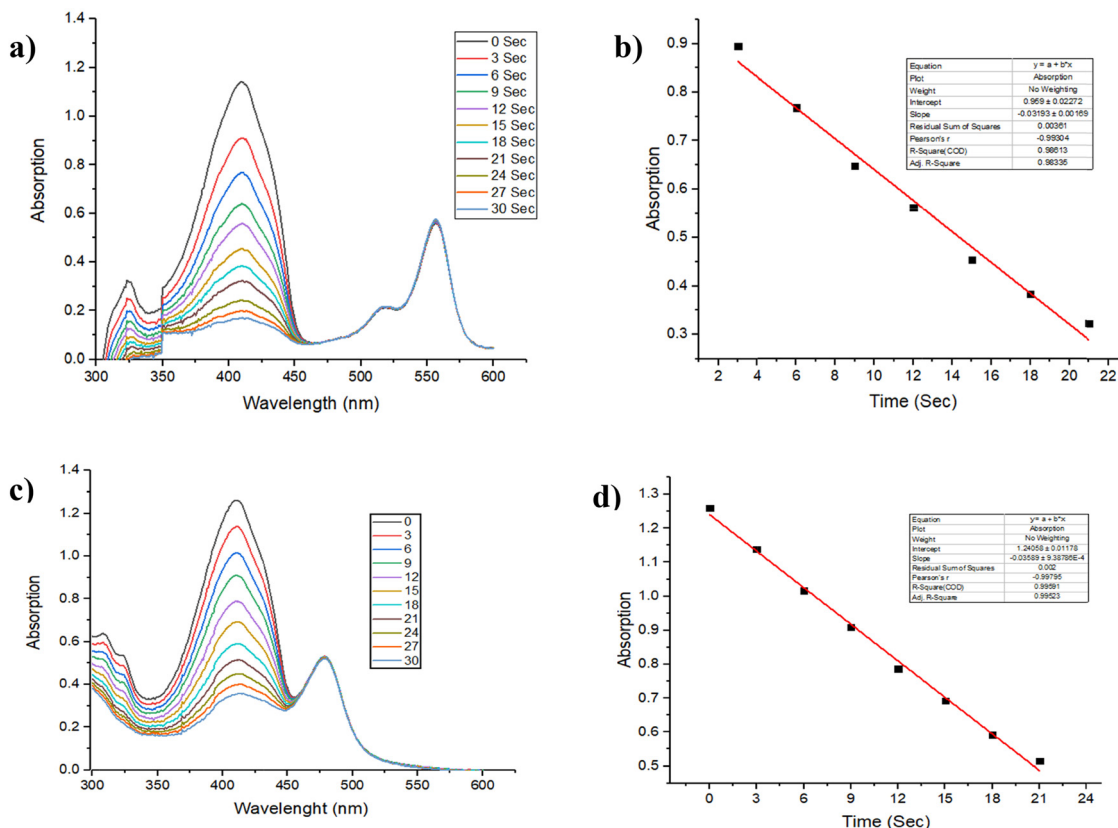**Fig. 1** Structures of Ir(III)dipyrrinato complexes.

Fig. 2 Singlet oxygen generation experiment and absorbance spectra of (a) Rose Bengal and (c) the **Ir3** complex upon irradiation of light (λ = 300–600 nm); rate of decrease of absorbance of DPBF at 411 nm by (b) Rose Bengal and (d) the **Ir3** complex.

Table 1 Optimization of the reaction conditions for photo-oxidative benzylamine coupling[a]

Entry	Light	Solvent	Catalyst	Yield[b] (%)
1	White	ACN	**Ir3**	97
2	White	ACN	**Ir2**	64
3	White	ACN	**Ir1**	84
4	Sunlight	ACN	**Ir3**	97
5	White	MeOH	**Ir3**	23
6	White	Hexane	**Ir3**	25
7	White	THF	**Ir3**	32
8	White	Chloroform	**Ir3**	54
9[c]	White	ACN	—	3
10[d]	—	ACN	**Ir3**	2

[a] Reaction conditions: benzylamine (1 mmol), solvent (4 mL), catalyst (0.05 mol%), irradiation of white light (24 W, 96 mW cm^{-2}) for 2 h under an O$_2$ atmosphere at rt. [b] Yield was calculated by ^{1}H-NMR using 1,3,5-trimethylbenzene (1 mmol) as an internal standard. [c] Time of reaction 12 h. [d] Time of reaction 12 h.
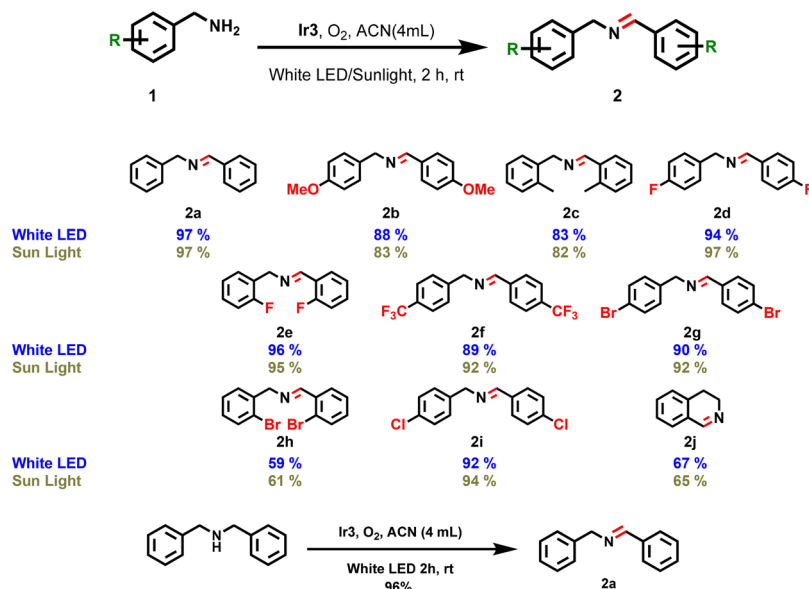
catalysts on the photocatalytic sulfoxidation of methylphenyl sulfide was systematically investigated (Table 2).

Initially, methanol (MeOH) was used as the solvent to assess the catalytic performance of various Ir(III)dipyrrinato photocatalysts. Among them, **Ir3** exhibited the highest efficiency,

affording the sulfoxide product in 98% yield (entry 2). **Ir1** and **Ir2** demonstrated moderate activity, yielding the product in 76% and 67% yield, respectively (entries 1 and 3). Subsequently, the effect of solvent variation was explored using **Ir3** as a photocatalyst. When the volume of MeOH was reduced to 4 mL, the product yield decreased to 64% (entry 4). Switching to ethanol (EtOH) as the solvent resulted in a slightly lower yield of 94% (entry 5), while the use of tetrahydrofuran (THF) and *N*,*N*-dimethylformamide (DMF) led to significantly lower conversions, affording the products in 12% and 17% yields, respectively (entries 6 and 7). Acetonitrile (ACN) demonstrated moderate efficiency, yielding 58% of the desired product (entry 8). In the absence of light and catalyst, only 2% and 4% yields were observed, respectively, confirming the necessity of light and photocatalysts for effective oxidation (entries 9 and 10). Light optimization (Table S1, ESI†) suggested that the white LED and sunlight work best for sulfoxidation reactions. These optimization results indicate that **Ir3** is most effective for sulfoxidation reactions, when exposed to white LED light or sunlight in methanol.

The substrate scope of the photocatalytic sulfoxidation reaction was explored using various substituted thioanisole derivatives under the optimized reaction conditions (Scheme 2). The reaction proceeded efficiently for substrates having electron-donating groups, such as methyl (**4b**, 97%/97%) and methoxy (**4c**, 83%/87%), yielding high conversion under white light and

Scheme 1 Substrate scope of benzylamine coupling.[a] [a] Reaction conditions: benzylamine (1 mmol), **Ir3** (0.05 mol%), solvent ACN (4 mL), irradiation with white light (24 W, 96 mW cm^{-2})/sunlight under an O$_2$ atmosphere at rt for 2 h.

Table 2 Catalyst and solvent optimization[a]

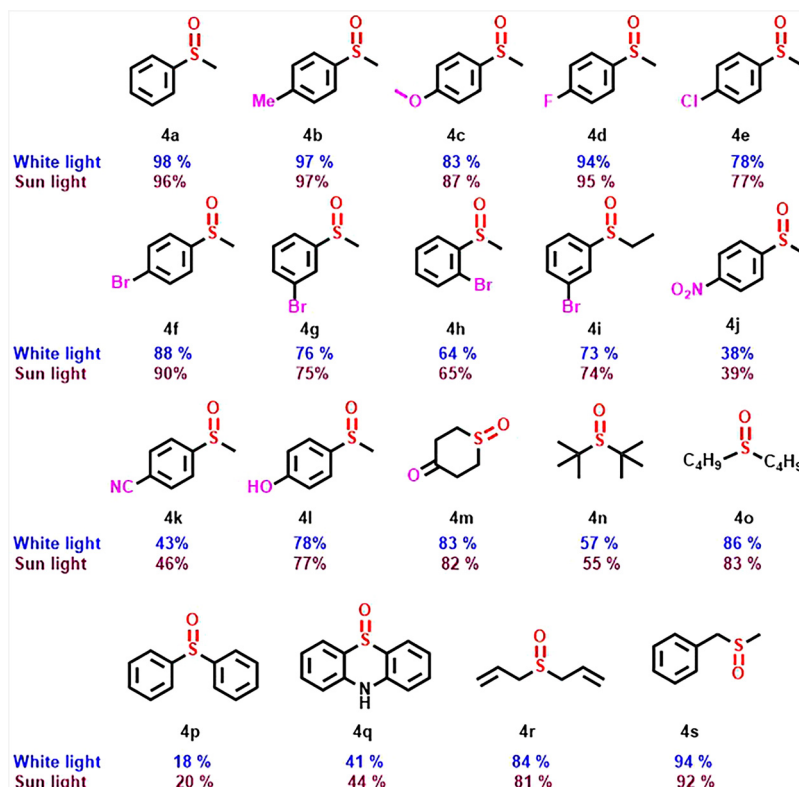| Entry	Solvent	Catalyst	Yield[b] (%)
1	MeOH 8 mL	**Ir1**	76
2	MeOH 8 mL	**Ir2**	67
3	MeOH 8 mL	**Ir3**	98
4	MeOH 4 mL	**Ir3**	64
5	EtOH 8 mL	**Ir3**	94
6	THF 8 mL	**Ir3**	12
7	DMF 8 mL	**Ir3**	17
8	ACN 8 mL	**Ir3**	58
9[c]	MeOH 8 mL	**Ir3**	2
10[d]	MeOH 8 mL	—	4

[a] Reaction conditions: methylphenyl sulfide (1 mmol), catalyst (0.05 mol%), irradiation with white light (24 W, 96 mW cm^{-2}) under an O$_2$ atmosphere at rt. [b] Yield was calculated by ^{1}H-NMR using 1,3,5-trimethylbenzene (1 mmol) as an internal standard. [c] No light reaction time 12 h. [d] No catalyst reaction time 12 h.

sunlight. Similarly, substrates containing halogen substituents, including fluorine (**4d**, 94%/95%), chlorine (**4e**, 78%/77%) and bromine (**4f**, 88%/90%), demonstrated good to excellent yields, indicating that halogenated substrates are well tolerated in the reaction, while the yield of *meta*-substituted (**4g**, 76%/75% and **4i**, 73%/74%) and *ortho*-substituted (**4h**, 64%/65%) bromine was lower compared to that of *para*-substituted (**4f**, 88%/90%) bromine, indicating a negative effect of steric hindrance on product yield. In contrast, substrates with electron-withdrawing groups, such as nitro (**4j**, 38%/39%) and cyano (**4k**, 43%/46%), provided lower yields. Diverse functional groups such as hydroxy-substituted compounds and heterocyclic sulfoxide also provided good

yields (**4l**, 77%/78%) and (**4m**, 82%/83%), respectively, in both sunlight and white light. The alkyl-substituted sulfides, including *tert*-butyl (**4n**, 57%/55%) and *n*-butyl (**4o**, 86%/83%), also demonstrated efficient photo-oxidation. Biphenyl thioether produced **4p** with a yield of only 18% in white light and 20% in sunlight, also indicating steric hindrance effects. In the case of phenothiazine, the product (**4q**) yield was only 41% and 44% in white light and sunlight, respectively. Also, diallylsulfane produces **4r** and benzyl(methyl)sulfane produces **4s** with excellent yields. In all cases, comparable yields were obtained under both white light and sunlight irradiation.

To understand the reaction mechanism, inhibition experiments were conducted (Table 3) in the case of KI, which is an inhibitor of h$^+$ (PC$^{+•}$).[24] The yield of sulfoxidation and benzylamine coupling reactions decreased to 36% and 6%, respectively (entry 1), which indicates that h$^+$ (PC$^{+•}$) is responsible for the product formation in both cases. In the presence of NaN$_3$ and benzoquinone, which act as scavengers of singlet oxygen (^{1}O$_2$)[44] and peroxide radicals (O$_2^{•-}$),[45] respectively (entries 1 and 2), a significant decrease in the yield of both products is observed, suggesting that both singlet oxygen (^{1}O$_2$) and peroxide radicals (O$_2^{•-}$) were involved in product formation.[45] The presence of thioether cationic radicals is also confirmed by 1,4-dimethoxy-benzene,[44] whereas no significant change in yield was observed in the presence of isopropanol, which suggests no involvement of the hydroxyl radical ($^•$OH) in the reaction mechanism.[46] With the help of these inhibition experiments, the following mechanism was proposed (Fig. 3), which indicates that the reaction follows both energy and electron transfer mechanisms. In the case of energy transfer, when light falls on the catalyst, it gets excited to a singlet excited state **Ir3***(S1) and, then through ISC, gets converted to a triplet excited state **Ir3***(T$_1$). The triplet excited state **Ir3***(T$_1$) reacts

Scheme 2 Substrate scope for the sulfoxidation reaction.[a] [a] Reaction conditions: sulfide (1 mmol), **Ir3** catalyst (0.05 mol%), solvent MeOH (8 mL), irradiation of white light (24 W, 96 mW cm^{-2})/sunlight under an O$_2$ atmosphere at rt for 2 h.

Table 3 Inhibition experiments in the presence of various scavengers[a]

Entry	Scavengers[c]	Inhibited species	Yield[b] (%) (sulfoxidation)	Yield[b] (%) (benzylamine coupling)
1	KI	PC$^{+\bullet}$ (h$^+$)	36	6
2	NaN$_3$	^{1}O$_2$	10	11
3	Benzoquinone	O$_2^{\bullet-}$	9	34
4[d]	1,4-Dimethoxy-benzene	Thioether cationic radical	65	—
5	Isopropanol	$^\bullet$OH	94	93

[a] Reaction conditions: methylphenyl sulfide/benzylamine (1.0 mmol), **Ir3** (0.05 mol%), MeOH/ACN 8/4 mL, irradiation with white light (24 W, 96 mW cm^{-2}) under an O$_2$ atmosphere at rt for 2 h. [b] ^{1}H-NMR yields. [c] Scavengers (1.0 mmol). [d] Only used in the sulfoxidation reaction.

with O$_2$ and forms singlet oxygen (^{1}O$_2$); when this ^{1}O$_2$ reacts with benzylamine, intermediate benzaldehyde is generated and then it reacts with another benzylamine to form the desired photocoupled imine product.

In the case of electron transfer, the excited state of the photocatalyst (**Ir3***) donates an electron to oxygen to generate an oxygen anionic radical (O$_2^{-\bullet}$) and **Ir3*** gets oxidised to **Ir3$^{+\bullet}$** which, upon reaction with benzylamine, generates an intermediate **I** and returns to its ground state (**Ir3**). Intermediate **I** reacts with O$_2^{-\bullet}$ and generates benzaldehyde. Then, benzaldehyde reacts with another benzylamine to form the desired imine. In the case of sulfoxidation, energy transfer and electron transfer mechanisms follow the same cycle until singlet oxygen (^{1}O$_2$) or the oxygen anionic radical (O$_2^{-\bullet}$) is generated. After that, singlet oxygen (^{1}O$_2$) and the oxygen anionic radical (O$_2^{-\bullet}$) react with thioether and intermediate **II**, respectively, which

generates an intermediate **III**. Then, another molecule of thioether reacts with intermediate III to form the desired sulfoxide.

Aerobic hydroxylation of boronic acids

Apart from benzylamine coupling and sulfoxidation, the aerobic hydroxylation of boronic acid was also catalysed by the Ir(III)dipyrrinato catalyst system. In this reaction, phenylboronic acid is converted into phenol in the presence of light, which is an additive that acts as a sacrificial electron transfer reagent and catalyst in open air only.

The influence of various additives and solvents on the photocatalytic aerobic hydroxylation of boronic acid was systematically investigated using different Ir(III)dipyrrinato photocatalysts (Table 4). When diethyl amine was used as an additive in acetonitrile (ACN), **Ir3** showed the highest catalytic efficiency,
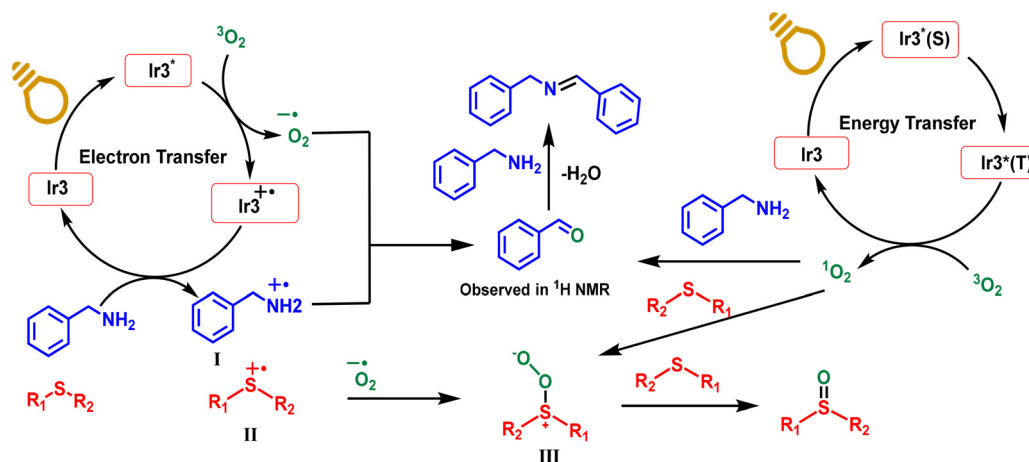
Fig. 3 Proposed mechanisms for visible light-induced oxidation of sulfides and oxidative benzylamine coupling using **Ir3** as a photosensitizer (PS) through both electron transfer and energy transfer.

affording product **6a** with 98% yield (entry 3). Under the same conditions, **Ir1** and **Ir2** demonstrated 75% and 48% product yields, respectively (entries 1 and 2). The role of different additives was further explored using **Ir3** in ACN. Triethylamine (TEA) facilitated the reaction efficiently, yielding 93% (entry 4), whereas diisopropylamine (DIPA) and triphenylamine led to significantly lower yields of 47% and 32%, respectively (entries 5 and 6). The effect of solvent was also examined using **Ir3** with diethyl amine as an additive. While the reaction proceeded efficiently in methanol (MeOH) and toluene, affording the product in 76% and 83% yields, respectively (entries 7 and 9), in the case of dimethyl sulfoxide (DMSO), only 5% product yield was observed (entry 8). Notably, when chloroform ($CHCl_3$) was

employed, an excellent yield of 96% was obtained (entry 10). When water is used for the reaction, the yield of the reaction decreases to 17% (entry 11). Notably, in the absence of a photocatalyst, no product formation was observed (entry 12), while without additives or without light, a negligible amount of product was observed (entries 13 and 14), which confirms that a catalyst, additive and white light are much needed for the reaction.

These findings established that **Ir3** as a photocatalyst, diethyl amine as an additive and ACN as a solvent in the presence of a white LED work best for the photocatalytic aerobic hydroxylation of boronic acid reaction.

The substrate scope of the photocatalytic hydroxylation of aryl boronic acids was investigated under the optimized conditions (Scheme 3). Electron-donating substituents, such as methoxy (**6a**, 98%) and methyl (**6b**, 96%), exhibited excellent yields, while in the case of *meta* (**6c**) and *ortho* (**6d**), methyl-substituted groups also showed good conversion with 89% and 83% yields, respectively. In contrast, the dimethoxy-substituted derivative (**6e**) showed only 57% yield. In the case of phenyl-boronic acid, phenol (**6f**) was produced with a 94% yield. Electron-withdrawing substituents such as nitrile (**6g**, 92%), nitro (**6h**, 91%) and trifluoromethyl (**6i**, 64%) groups were well tolerated and gave good to excellent yields, while halogens, including chloro (**6j**, 91%) and bromo (**6k**, 80%), maintained high reactivity. Functionalized substrates with ketone (**6l**, 87%), carboxylic acid (**6m**, 94%), ethyl ester (**6n**, 90%) and aldehydes (**6o**, 78%) demonstrated excellent reactivity, while extended aromatic systems, such as naphthalene-derivatives resulted hydroxylation product (**6p**, 45%) and (**6q**, 53%), in moderate yields. Overall, the results demonstrate the broad functional group tolerance of the photocatalytic hydroxylation system, making it a versatile approach for the selective hydroxylation of aryl boronic acids.
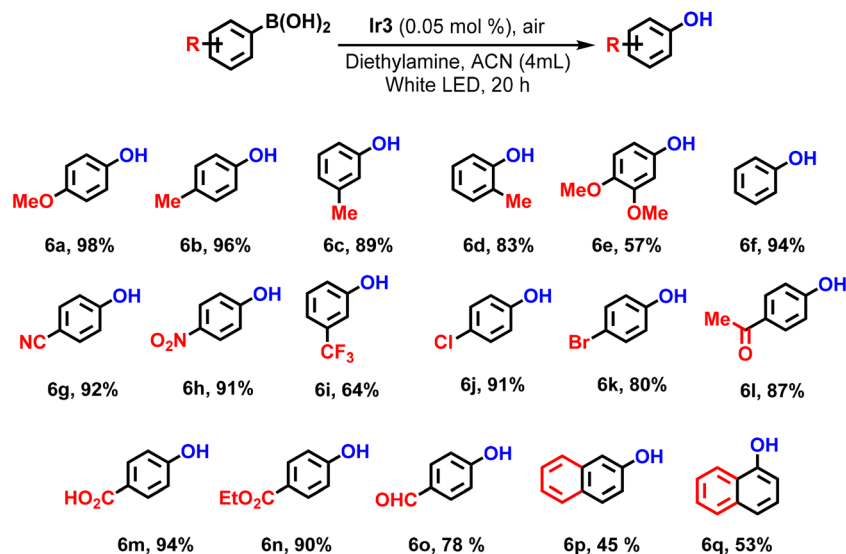
In the past, Ir or Ru cyclometalated complexes were employed for similar reactions. In Table 5 the results from this work are compared with those of the previously reported

Table 4 Optimization of the reaction conditions for aerobic hydroxylation of boronic acid[a]

Entry	Catalyst	Additive	Solvent	Yield[b] (%)
1	**Ir1**	Diethyl amine	ACN	75
2	**Ir2**	Diethyl amine	ACN	48
3	**Ir3**	Diethyl amine	ACN	98
4	**Ir3**	TEA	ACN	93
5	**Ir3**	DIPA	ACN	47
6	**Ir3**	Triphenyl amine	ACN	32
7	**Ir3**	Diethyl amine	MeOH	76
8	**Ir3**	Diethyl amine	DMSO	5
9	**Ir3**	Diethyl amine	Toluene	83
10	**Ir3**	Diethyl amine	$CHCl_3$	96
11	**Ir3**	Diethyl amine	H_2O	17
12	No catalyst	Diethyl amine	ACN	—
13	**Ir3**	—	ACN	3
14[c]	**Ir3**	Diethyl amine	ACN	2

[a] Reaction conditions: (4-methoxyphenyl)boronic acid (0.5 mmol), catalyst (0.05 mol%), additive (1 mmol), solvent (4 mL), irradiation with white light (24 W, 96 mW cm^{-2}) in the open air at rt for 20 h. [b] Isolated from column chromatography. [c] No light.

Scheme 3 Substrate scope for the aerobic hydroxylation of boronic acid.[a] [a] Reaction conditions: boronic acid (0.5 mmol), catalyst **Ir3** (0.05 mol%), diethylamine (1 mmol), ACN (4 mL), irradiation with white light (24 W, 96 mW cm^{-2}) in open air at rt for 20 h.

Table 5 Comparison between various catalytic systems and the current catalyst

Ref.	Reaction	Catalyst	Catalytic loading (mol%)	Time (h)	Maximum yield (%)
32	Benzylamine coupling	Ir(III) based catalyst	0.25	5	92
26	Sulfoxidation	Rose Bengal	2	6–48	99
		Ru(bpy)$_3$$^{2+}$	2	24	50
		Ir(ppy)$_3$	2	24	—
29	Sulfoxidation	Ir(III) based catalyst	0.5	4	98
37	Hydroxylation of aryl boronic acids	Ir(ppy)$_3$	2	84	90
		Ru(bpy)$_3$$^{2+}$	2	26	96
36	Hydroxylation of aryl boronic acids	Ir(III) based catalyst	2	5–12	95
This work	Benzylamine coupling	**Ir3**	0.05 mol%	2	97
	Sulfoxidation	**Ir3**	0.05	2	98
	Hydroxylation of aryl boronic acids	**Ir3**	0.05	20	98

catalysts. It is clear that previous systems used a higher amount of catalyst loading (0.25–2 mol%), whereas the Ir(III)dipyrrinato catalyst works very well at lower catalytic loading (0.05 mol%) with a reduced reaction time.

Conclusion

In summary, Ir(III)dipyrrinato complexes have proven to be highly efficient photocatalysts for aerobic oxidation reactions, including photo-oxidative benzylamine coupling, oxidation of sulfides to sulfoxides and the hydroxylation of aryl boronic acids. These reactions proceed with excellent yields within a short reaction time, showcasing the high reactivity and efficiency of these complexes. The exceptional singlet oxygen generation quantum yields, long-lived triplet excited states and strong visible-light absorption make these complexes particularly well-suited for photochemical applications. Furthermore, the remarkably low catalyst loading of only 0.05 mol% compared to other catalytic systems highlights their cost-effectiveness and sustainability. The broad substrate tolerance and versatility of these systems provide an effective strategy for synthesizing diverse functionalized organic molecules.

Experimental section

General procedure for the photocatalytic benzylamine coupling reaction

Benzylamine (1 mmol) and the Ir(III)dipyrrinato catalyst (0.05 mol%) were dissolved in acetonitrile and added to a 10 mL borosilicate round-bottom flask. The solution was periodically saturated with oxygen by slow purging with a long needle every hour. The reaction mixture was stirred at room temperature and irradiated using a Smartchem Synth Photo-reactor (24 W, white LED) for 2 hours. The reaction progress was monitored *via* ^{1}H NMR. Upon completion, the product was purified using basic silica gel column chromatography with hexane/ethyl acetate as an eluent and subsequently characterized by ^{1}H and ^{13}C NMR spectroscopy using a Bruker Avance-500 MHz spectrometer.

General procedure for the sulfoxidation reaction

Sulfide (1 mmol) and the Ir(III)dipyrrinato catalyst (0.05 mol%) were dissolved in methanol and added to a 25 mL borosilicate round-bottom flask. To ensure oxygen saturation, the solution was gently purged with oxygen using a long needle every hour

for 15–20 minutes. The reaction mixture was stirred at room temperature while being irradiated with a Smartchem Synth Photoreactor (24 W, white LED) for 2 hours. After completion, the product was purified using silica gel column chromatography with a hexane/ethyl acetate/methanol eluent system. The purified compound was then characterized by ^{1}H and ^{13}C NMR spectroscopy using a Bruker Avance-500 MHz spectrometer.

General procedure for photocatalytic aerobic hydroxylation of boronic acid

Boronic acid (0.5 mmol), additive (1 mmol) and the Ir(III)di-pyrrinato catalyst (0.05 mol%) were dissolved in 4 mL of acetonitrile and added to a 10 mL borosilicate round-bottom flask in open air. The reaction mixture was stirred at room temperature and irradiated using a Smartchem Synth Photo-reactor (24 W, white LED) for 20 hours. The reaction progress was monitored via thin-layered chromatography. Upon completion, the product was purified using basic silica gel column chromatography with hexane/ethyl acetate as an eluent and subsequently characterized by ^{1}H and ^{13}C NMR spectroscopy using a Bruker Avance-500 MHz spectrometer.

Data availability

All data will be made available on request, and the supporting data have been included as part of the ESI.†

Conflicts of interest

No conflict of interest is declared.

Acknowledgements

References

1 S. Murahashi, Angew. Chem., Int. Ed. Engl., 1995, 34, 2443–2465.

2 S. Kobayashi, Y. Mori, J. S. Fossey and M. M. Salter, Chem. Rev., 2011, 111, 2626–2704.

3 J. H. P. Tyman, Synthetic and natural phenols, Elsevier, 1996, vol. 52.

4 A. Kotschy and G. Timári, Heterocycles from transition metal catalysis: formation and functionalization, Springer Science & Business Media, 2005, vol. 28.

5 C. A. Fyfe, The Chemistry of the Hydroxyl Group, ed. S. Patai, Wiley-Interscience, New York, 1971, vol. 1.

6 Z. V. I. Rappoport, The chemistry of phenols, John Wiley & Sons, 2004.

7 K. C. Nicolaou, C. J. N. Mathison and T. Montagnon, Angew. Chem., Int. Ed., 2003, 42, 4077–4082.

8 H. Pellissier, Tetrahedron, 2006, 62, 5559–5601.

9 I. Fernández and N. Khiar, Chem. Rev., 2003, 103, 3651–3706.

10 R. A. Volkmann, Comprehensive Organic Synthesis, Oxford, 1st edn, 1991.

11 J. Legros, J. Dehli and C. Bolm, Adv. Synth. Catal., 2005, 347, 19–31.

12 E. Skolia, P. L. Gkizis and C. G. Kokotos, ChemPlusChem, 2022, 87, e202200008.

13 C. G. Overberger and R. W. Cummins, J. Am. Chem. Soc., 1953, 75, 4250–4254.

14 R. Curci, R. DiPrete, J. O. Edwards and G. Modena, J. Org. Chem., 1970, 35, 740–745.

15 V. G. Shukla, P. D. Salgaonkar and K. G. Akamanchi, J. Org. Chem., 2003, 68, 5422–5425.

16 B. Yu, A.-H. Liu, L.-N. He, B. Li, Z.-F. Diao and Y.-N. Li, Green Chem., 2012, 14, 957.

17 C. K. Prier, D. A. Rankic and D. W. C. MacMillan, Chem. Rev., 2013, 113, 5322–5363.

18 A. Jain, S. Kumar, Sanyam, A. Mondal and I. Gupta, J. Catal., 2024, 438, 115705.

19 K. L. Skubi, T. R. Blum and T. P. Yoon, Chem. Rev., 2016, 116, 10035–10074.

20 M. Fagnoni, D. Dondi, D. Ravelli and A. Albini, Chem. Rev., 2007, 107, 2725–2756.

21 A. Jain and I. Gupta, SynOpen, 2024, 8, 153–168.

22 A. Sridhar, R. Rangasamy and M. Selvaraj, New J. Chem., 2019, 43, 17974–17979.

23 Y. Zou, J. Chen, X. Liu, L. Lu, R. L. Davis, K. A. Jørgensen and W. Xiao, Angew. Chem., 2012, 3, 808–812.

24 J. Jiang, R. Luo, X. Zhou, Y. Chen and H. Ji, Adv. Synth. Catal., 2018, 360, 4402–4411.

25 H. Nai, J. Hou, J. Li, X. Ma, Y. Yang, K. Qu, X. Huang and L. Li, RSC Adv., 2024, 14, 7924–7931.

26 X. Gu, X. Li, Y. Chai, Q. Yang, P. Li and Y. Yao, Green Chem., 2013, 15, 357–361.

27 A. Casado-Sánchez, R. Gómez-Ballesteros, F. Tato, F. J. Soriano, G. Pascual-Coca, S. Cabrera and J. Alemán, Chem. Commun., 2016, 52, 9137–9140.

28 J. Dad'ová, E. Svobodová, M. Sikorski, B. König and R. Cibulka, ChemCatChem, 2012, 4, 620–623.

29 S. Li, L. Li, Y. Li, L. Dai, C. Liu, Y. Liu, J. Li, J. Lv, P. Li and B. Wang, ACS Catal., 2020, 10, 8717–8726.

30 E.-T. Wu and M. H. Huang, ACS Catal., 2023, 13, 14746–14752.

31 J. Jin, H. W. Shin, J. H. Park, J. H. Park, E. Kim, T. K. Ahn, D. H. Ryu and S. U. Son, Organometallics, 2013, 32, 3954–3959.

32 L. P. Li and B. H. Ye, Inorg. Chem., 2019, 58, 7775–7784.

33 L. Hao, G. Ding, D. A. Deming and Q. Zhang, Eur. J. Org. Chem., 2019, 7307–7321.

34 Y. Wan, X. Li, J. Ma and G. Zhang, Eur. J. Org. Chem., 2025, e202401152.

35 D. A. Nicewicz and T. M. Nguyen, ACS Catal., 2014, 4, 355–360.

36 H. Yu, C. Liu, X. Dai, J. Wang and J. Qiu, *Tetrahedron*, 2017, **73**, 3031–3035.

37 Y. Q. Zou, J. R. Chen, X. P. Liu, L. Q. Lu, R. L. Davis, K. A. Jørgensen and W. J. Xiao, *Angew. Chem., Int. Ed.*, 2012, **51**, 784–788.

38 N. Manav, R. Singh, A. Janaagal, A. K. S. Yadav, V. Pandey and I. Gupta, *New J. Chem.*, 2022, **46**, 19310–19321.

39 S. Kumar, K. Agarwal, Sanyam, A. Mondal and I. Gupta, *Chem. – Asian J.*, 2024, **19**, e202400680.

40 H. Zhang, H. Wang, K. Tanner, A. Schlachter, Z. Chen, P. D. Harvey, S. Chen and W. Y. Wong, *Dalton Trans.*, 2021, **50**, 10629–10639.

41 N. Manav, M. Y. Lone, M. K. Raza, J. Chavda, S. Mori and I. Gupta, *Dalton Trans.*, 2022, **51**, 3849–3863.

42 V. Pandey, A. Janaagal, A. Jain, S. Mori and I. Gupta, *Dyes Pigm.*, 2023, **209**, 110861.

43 F. Wilkinson, W. P. Helman and A. B. Ross, *J. Phys. Chem. Ref. Data*, 1993, **22**, 113–262.

44 S. Lacombe and T. Pigot, *Catal. Sci. Technol.*, 2016, **6**, 1571–1592.

45 S. M. Bonesi, I. Manet, M. Freccero, M. Fagnoni and A. Albini, *Chem. – Eur. J.*, 2006, **12**, 4844–4857.

46 E. Baciocchi, T. Del Giacco, F. Elisei, M. F. Gerini, M. Guerra, A. Lapi and P. Liberali, *J. Am. Chem. Soc.*, 2003, **125**, 16444–16454.